

Direct Lens Imaging of Galactic Bulge Microlensing Events

Cheongho Han[†] & Heon-Young Chang^{‡★}

[†]*Department of Physics, Institute for Basic Science Research, Chungbuk National University, Chongju 361-763, Korea*

[‡]*Korea Institute for Advanced Study, 207-43 Cheongryangri-dong Dongdaemun-gu, Seoul 130-012, Korea*

4 June 2005

ABSTRACT

Recently, from the *Hubble Space Telescope* (HST) images of one of the Large Magellanic Cloud (LMC) events taken 6.3 years after the original lensing measurement, Alcock et al. were able to directly image the lens. Although the first resolved lens was identified for an LMC event, much more numerous lenses are expected to be resolved for Galactic bulge events. In this paper, we estimate the fraction of Galactic bulge events whose lenses can be directly imaged under the assumption that all bulge events are caused by normal stars. For this determination, we compute the distribution of lens proper motions of the currently detected Galactic bulge events based on standard models of the geometrical and kinematical distributions of lenses and their mass function. We then apply realistic criteria for lens resolution, and the result is presented as a function of the time elapsed after an original lensing measurement, Δt . If followup observations are performed by using an instrument with a resolving power of $\theta_{\text{PSF}} = 0''.1$, which corresponds to that of HST equipped with the new Advanced Camera for Surveys, we estimate that lenses can be resolved for $\sim 3\%$ and 22% of disk-bulge events and for $\sim 0.3\%$ and 6% of bulge self-lensing events after $\Delta t = 10$ and 20 years, respectively. The fraction increases substantially with the increase of the resolving power. If the instrument has a resolution of $\theta_{\text{PSF}} = 0''.05$, which can be achieved by the *Next Generation Space Telescope*, we estimate that lenses can be resolved for $\sim 22\%$ and 45% of disk-bulge events and for $\sim 6\%$ and 23% of bulge self-lensing events after $\Delta t = 10$ and 20 years, respectively.

Key words: gravitational lensing – stars: fundamental parameters

★ e-mails: cheongho@astroph.chungbuk.ac.kr (CH); hyc@ns.kias.re.kr (HYC)

1 INTRODUCTION

Following the proposal of Paczyński (1986), experiments to search for lensing-induced light variations of stars (microlensing events) located in the Galactic bulge and the Magellanic Clouds have been or are being conducted by several groups (MACHO: Alcock et al. 1993; EROS: Aubourg et al. 1993; OGLE: Udalski et al. 1993; MOA: Bond et al. 2001; DUO: Alard & Guibert 1997). These experiments have successfully detected a large number of events ($\sim 1,000$), most of which are detected towards the Galactic bulge.

Despite a large number of event detections, the nature of the lenses is still poorly known. This is because the Einstein ring radius crossing time t_E (Einstein timescale), which is the only observable providing information about the physical parameters of the lens (lens parameters), results from a combination of the lens parameters, i.e.

$$t_E = \frac{r_E}{v}; \quad r_E = \left[\frac{4GM}{c^2} \frac{D_{OL}(1 - D_{OL})}{D_{OS}} \right]^{1/2}, \quad (1)$$

where r_E is the Einstein ring radius, M is the lens mass, v is the lens-source transverse speed, and D_{OL} and D_{OS} are the distances to the lens and the source from the observer, respectively. Under this circumstance, the only approach one could pursue would be identifying the major lens population by statistically determining the lens mass function based on the observed timescale distribution. However, this approach requires *a priori* knowledge about the geometrical distribution of the lens, the lens kinematics, and the functional form of the lens mass function, which are all poorly known. In addition, even if all lensing objects were of the same mass, they would give rise to a broad range of timescale. As a result, it is difficult to identify the major lens population from this approach (Mao & Paczyński 1996; Gould 2001).

Recently, from the *Hubble Space Telescope* (HST) images of one of the Large Magellanic Cloud (LMC) events (MACHO LMC-5) taken 6.3 years after the original lens measurement, Alcock et al. (2001) were able to resolve the lens from the lensed source star. By directly imaging the lens, they could identify that the event was caused by a nearby low mass star located in the Galactic disk.

Besides the identification of the lens as a normal star, direct lens imaging is of scientific importance due to following reasons. First, by directly and accurately measuring the lens proper motion with respect to the source, μ , one can better constrain the physical parameters of the individual lenses. The previous method to determine μ is based on the analysis of the lensing light curves of events affected by the finite source effect, such as source-transit single lens events and caustic-crossing binary lens events (Gould 1994; Witt & Mao 1994; Nemiroff & Wickramasinghe 1994). By analyzing the part of the light curves near the source transit or the caustic crossing of these events, one can measure the source star angular radius

normalized by the angular Einstein ring radius θ_E , i.e. $\rho_\star = \theta_\star/\theta_E$, where θ_\star is the angular source star radius. Then, the lens proper motion is determined by

$$\mu = \frac{\theta_E}{t_E} = \frac{\theta_\star/\rho_\star}{t_E}. \quad (2)$$

For the proper motion determination by using this method, however, one should know the source star angular radius, which can only be deduced from an uncertain color-surface brightness relation. As a result, the proper motions determined in this way suffer from large uncertainties. By contrast, if the lens is resolved, the proper motion can be directly and thus accurately measured from the observed image. Measuring the proper motion is equivalent to measuring the angular Einstein ring radius because $\theta_E = \mu t_E$, where the event timescale is determined from the light curve. While t_E depends on three lens parameters of M , D_{OL} , and v , θ_E does not depend on v , and thus the lens mass can be better constrained. Second, if the lens is resolved for an event where the lens-source relative parallax, $\pi_{\text{rel}} = \text{AU}/(D_{OL}^{-1} - D_{OS}^{-1})$, was previously measured during the lensing magnification, one can completely break the lens parameter degeneracy and the lens mass is uniquely determined by

$$M = \frac{\mu^2 t_E^2}{\kappa \pi_{\text{rel}}}, \quad (3)$$

where $\kappa = 4G/(c^2 \text{AU}) \sim 8.144 \text{ mas}/M_\odot$ (Gould 2001). Third, if the source of an event was resolved via either a source transit or a caustic crossing and thus ρ_\star was precisely measured, one can determine the angular source star radius by reversing the process of the classical method of the proper motion determination, i.e. $\theta_\star = \mu t_E \rho_\star$. By measuring θ_\star , one can determine the effective temperature of the source star, which is important for the accurate construction of stellar atmosphere models (e.g., Alonso et al. 2000).

Although the first directly imaged lens was identified for an LMC event, much more numerous direct lens identifications are expected if high resolution followup observations are performed for events detected towards the bulge. There are several reasons for this expectation. First, compared to the total number of LMC events, which is ~ 20 , there are an overwhelmingly large number of bulge events. Second, while the majority of LMC events are suspected to be caused by dark (or very faint) objects, most bulge events are supposed to be caused by normal stars, for which imaging is possible. Third, an important fraction of lenses responsible for bulge events are believed to be located in the Galactic disk with moderate distances, and thus more likely to be imaged due to their tendency of being bright and having large proper motions.

The goal of this work is to estimate the fraction of Galactic bulge events whose lenses can be directly imaged. For this estimation, we first compute the expected distribution of the lens-source proper motions of the currently detected Galactic bulge events based on standard models of the geometrical and kinematical distributions of lenses and their mass function (§ 2). We then apply realistic detection criteria for lens resolution and the result is

presented as a function of the time elapsed after the original lensing measurement, Δt (§ 3). Based on the result in § 3, we discuss some of the observational aspects of the future high resolution followup lensing observations aimed for direct lens imaging (§ 4). We summarize the result and conclude in § 5.

2 PROPER MOTIONS

The first requirement for direct lens imaging is that the lens should have a large relative proper motion with respect to the source so that it can be widely separated from the lensed source star within a reasonable amount of Δt . In this section, we, therefore, estimate the expected distribution of proper motions of Galactic bulge events.

With the models of the lens mass function, $\phi(M)$, the matter density distributions of the lens and source stars along the line of sight towards the Galactic bulge field, $\rho(D_{\text{OL}})$ and $\rho(D_{\text{OS}})$, and the kinematical distribution of lens-source transverse velocities, $f(\mathbf{v})$, the distribution of lens proper motions of Galactic bulge events is computed by

$$\begin{aligned} \Gamma(\mu) \propto & \int_0^\infty dD_{\text{OS}} \rho(D_{\text{OS}}) \int_0^{D_{\text{OS}}} dD_{\text{OL}} \rho(D_{\text{OL}}) \\ & \times \int_0^\infty \int_0^\infty dv_y dv_z v f(v_y, v_z) \\ & \times \int_0^\infty dM \phi(M) r_E \epsilon(t_E) \delta(\mu - v/D_{\text{OL}}), \end{aligned} \quad (4)$$

where v_y and v_z are the components of the transverse velocity which are respectively parallel with and normal to the Galactic disk plane, $\epsilon(t_E)$ is the detection efficiency of events as a function of t_E , and the notation $\delta(\cdot \cdot \cdot)$ represents the Dirac delta function. We note that the factors v and r_E are included in equation (4) to weight the event rate by the transverse speed and the lensing cross section.

For the Galactic bulge and disk matter density distributions, we adopt the models of Dwek et al. (1995) and Bahcall (1986), respectively. In the bulge model, the bulge has a triaxial shape and the matter density is represented by an analytic form of

$$\rho(r_s) \propto \exp(0.5r_s^2); \quad r_s^4 = [(x'/x_0)^2 + (y'/y_0)^2]^2 + (z'/z_0)^4, \quad (5)$$

where $(x_0, y_0, z_0) = (1.58, 0.62, 0.43)$ kpc, and the coordinates (x', y', z') represent the axes of the triaxial bar from the longest to the shortest, and the longest axis is misaligned with the line of sight toward the Galactic center by an angle $\theta = 20^\circ$. The Bahcall disk model is expressed by a double exponential form of

$$\rho(R, z) \propto \exp \left[- \left(\frac{R - 8000}{h_R} + \frac{z}{h_z} \right) \right], \quad (6)$$

where the radial scale length and the vertical scale height are $h_z = 325$ pc and $h_R = 3.5$ kpc, respectively.

For the transverse velocity distribution, we adopt the model of Han & Gould (1995). In

this model, the velocity distributions for both disk and bulge components have a Gaussian form of

$$f(v_i) \propto \exp \left[-\frac{(v_i - \bar{v}_i)^2}{2\sigma_i^2} \right], \quad i \in y, z. \quad (7)$$

The means and the standard deviations of the individual velocity components for events with disk lenses and bulge source stars (disk-bulge events) are

$$\begin{aligned} (\bar{v}_y, \sigma_y) &= (220.0, 30.0) \text{ km s}^{-1}, \\ (\bar{v}_z, \sigma_z) &= (0.0, 20.0) \text{ km s}^{-1}, \end{aligned} \quad (8)$$

where $\bar{v}_y = 220 \text{ km s}^{-1}$ corresponds to the rotation speed of the Galactic disk and $(\sigma_y, \sigma_z) = (30, 20) \text{ km s}^{-1}$ are the adopted velocity dispersions of stars in the solar neighborhood. For events with bulge source stars lensed by another foreground bulge stars (bulge self-lensing events), the means and standard deviations of the transverse velocity distributions are

$$\begin{aligned} (\bar{v}_y, \sigma_y) &= (0.0, 82.5) \text{ km s}^{-1}, \\ (\bar{v}_z, \sigma_z) &= (0.0, 66.3) \text{ km s}^{-1}. \end{aligned} \quad (9)$$

For the barred bulge, the velocity dispersions along the axes of the bar are deduced from the tensor virial theorem (Binney & Tremaine 1987), resulting in $(\sigma_{x'}, \sigma_{y'}, \sigma_{z'}) = (113.6, 77.4, 66.3) \text{ km s}^{-1}$. Due to the projection effect caused by the bar misalignment, the projected velocity dispersions are computed by $(\sigma_y, \sigma_z) = ([\sigma_{x'}^2 \sin^2 \theta + \sigma_{y'}^2 \cos^2 \theta]^{1/2}, \sigma_{z'}) = (82.5, 66.3) \text{ km s}^{-1}$, which correspond to the standard deviations in (9). We note that the adopted velocity model is a rough approximation in the sense that it does not include factors such as the systematic mean motion of bulge stars discussed by Evans & Belokurov (2002), the figure rotation of the bulge discussed by Blum (1995), and the possibility of non-Gaussian nature of disk star velocity distribution discussed by Evans & Collett (1993), which may actually be important in the resulting distribution of proper motions. Since the inclusion of the mean motion or the figure rotation of bulge stars result in high proper motions, we note that the fraction of resolvable lenses predicted by the adopted bulge velocity model is the lower limit.

The Einstein timescale distribution of events observed by the MACHO group is claimed to be consistent with the distribution from normal stars (Alcock et al. 2000b). We, therefore, model the mass function of lenses based on the present day main-sequence stars determined by Kroupa, Tout & Gilmore (1993). The adopted mass function has a three power-law functional form of

$$\phi(M) \propto \begin{cases} M^{-1.3} & \text{for } 0.08 M_\odot \leq M < 0.5 M_\odot \\ M^{-2.2} & \text{for } 0.5 M_\odot \leq M < 1.0 M_\odot \\ M^{-4.5} & \text{for } M \geq 1.0 M_\odot. \end{cases} \quad (10)$$

For the detection efficiency, we adopt the latest determination of the MACHO experiment (Alcock et al. 2000b), whose data were analyzed by using the ‘difference image analysis’ method.

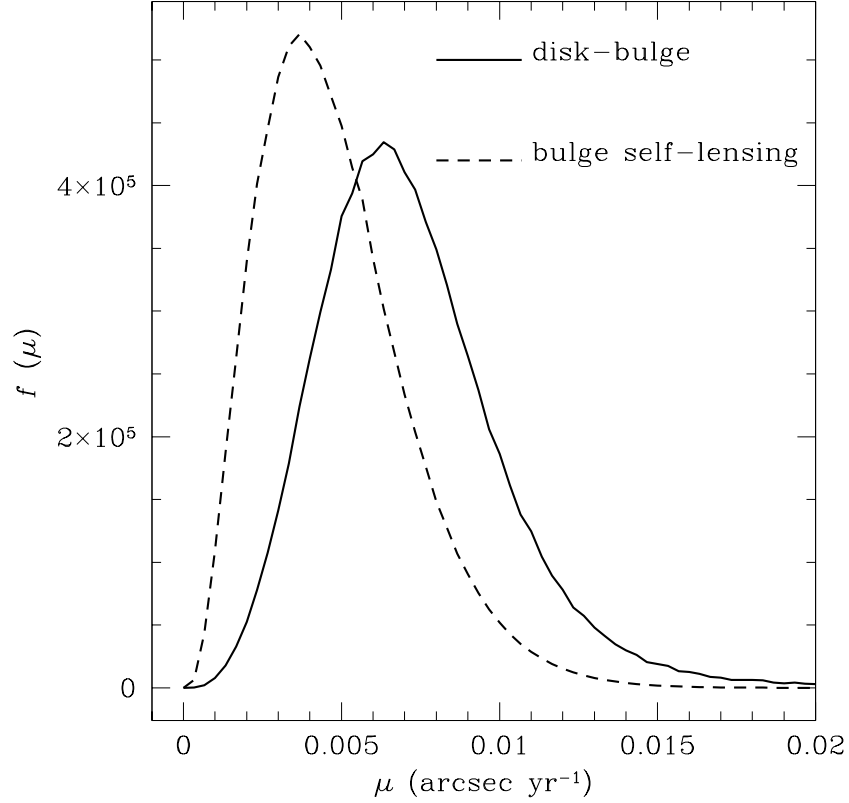


Figure 1. The expected distributions of relative lens-source proper motions for Galactic bulge events. The solid curve is for events with disk lenses and bulge source stars (disk-bulge events), while the dashed curve is for events with bulge source stars lensed by another foreground bulge stars (bulge self-lensing events). The ordinate of each distribution is arbitrarily normalized so that the areas under the two curves match together.

In Figure 1, we present the obtained distributions of relative lens-source proper motions for disk-bulge (solid curve) and bulge self-lensing (dashed curve) events, respectively. Due to the large uncertainties in the geometrical and kinematical distributions of lenses, the relative contribution of the disk and bulge lenses to the total event rate is very uncertain. We, therefore, leave the proper motion distributions of the disk-bulge and bulge self-lensing events separately, instead of estimating the distribution of total events by arbitrarily normalizing the ratio between the two populations of events. From the figure, one finds that, as expected, the average proper motion of events caused by disk lenses is larger than that of events caused by bulge lenses.

3 FURTHER RESTRICTION

The lens detectability is additionally restricted by the lens brightness. This is not only simply because the lens should be brighter than a detection limit, but also because the threshold lens-source separation for lens detection, θ_{th} , varies depending on the apparent lens/source flux ratio. Therefore, we compute the angular threshold as a function of the magnitude difference between the lens and the source, $\Delta m = m_L - m_S$.

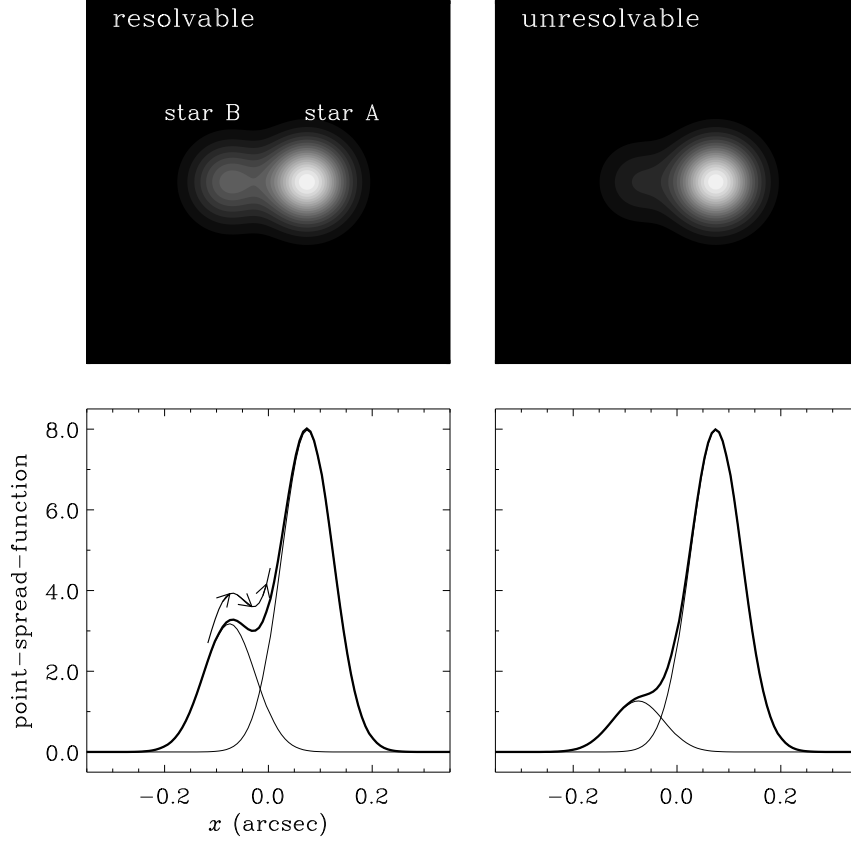


Figure 2. Criterion for resolving two closely located stars. The presented in each of the upper panels is the combined image of two stars and the thick solid curve in the corresponding lower panel is the one-dimensional PSF profile of the combined image. The two stars comprising the individual combined images have a common separation of $0''.15$, but have different magnitude differences of $\Delta m = 1.0$ (left image) and 2.0 (right image). The PSF of each star (thin solid curves in each of the lower panels) is modeled by a Gaussian, where the standard deviation σ represents the resolving power of the instrument to be used for imaging. Here we assume $\sigma = 0''.05$. We assume that the individual stars are resolved if the sign of the combined image's PSF profile changes more than twice in the overlapping region between the centers of the individual stellar images. Under this criterion, the two stars in the left panel is resolved, while the stars in the right panel is not resolved.

For the computation of $\theta_{\text{th}}(\Delta m)$, we first model the point-spread-function (PSF) of a stellar image as a Gaussian, where the standard deviation σ of the PSF characterizes the resolving power of the instrument to be used for followup lensing observations. We then generate the combined image of the lens and the source by normalizing such that the volume under each PSF is proportional to the flux of each star. Once the combined image is constructed, we then judge whether the lens and the source can be resolved each other. For this judgment, we assume that the lens can be resolved if the sign of the derivative of the combined image's one-dimensional PSF profile changes more than two times in the overlapping region between the centers of the lens and the source images (see Figure 2 for illustration). Then, the angular threshold is defined as the lens-source separation at which the lens is just to be resolved from the source star.

In Figure 3, we present the computed angular threshold as a function of Δm . The two curves correspond to the distributions expected when the followup observations are

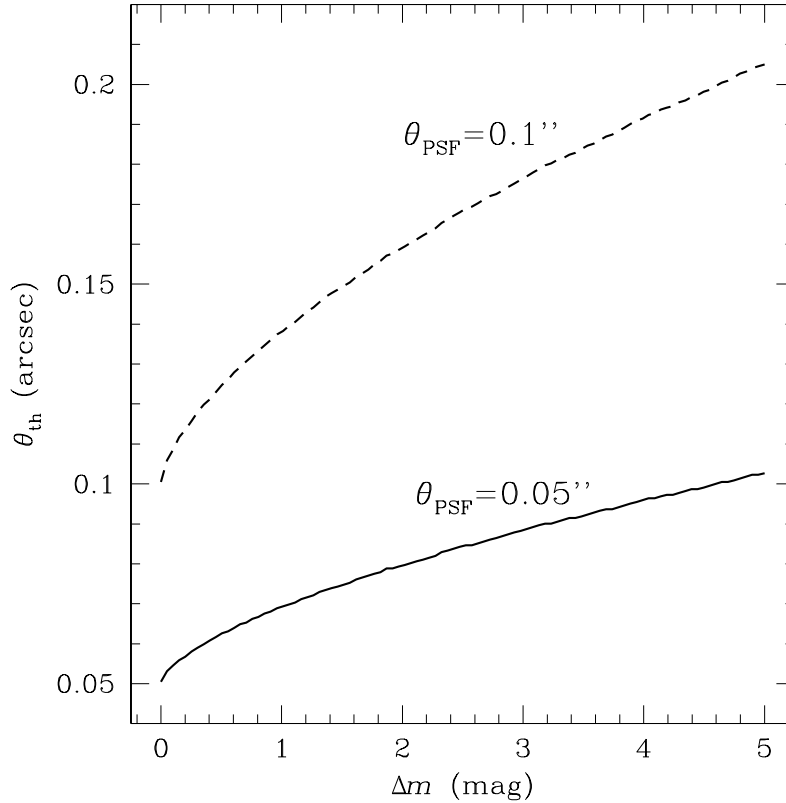


Figure 3. The threshold angular separation for resolving two closely located stars as a function of magnitude difference between the two stars. The angular threshold is computed for two instruments whose resolving power is characterized by $\theta_{PSF} = 0''.1$ and $\theta_{PSF} = 0''.05$.

carried out by using two different instruments, whose resolving powers are characterized by $\theta_{PSF} = 2\sigma = 0''.1$ (dashed curve) and $0''.05$ (solid curve), respectively. We note that the Advanced Camera for Surveys (ACS) recently installed on HST can achieve a resolution of $\theta_{PSF} \sim 0''.1$. We also note that the Near Infrared Camera (NIRCam) of *Next Generation Space Telescope* (NGST), which will have an aperture of 6 – 7 m, will be sensitive in the wavelength range of 0.6 to 5 microns, and thus can achieve $\theta_{PSF} \sim 0''.05$. From the figure, one finds that as the lens becomes fainter, it becomes difficult to resolve the lens from the source star.

With the computed distribution of $\theta_{th}(\Delta m)$, we recalculate the distribution of proper motions of events by using equation (4), but in this time only for events with detectable lenses. To be detected, the lens should meet the condition of $\mu\Delta t \geq \theta_{th}(\Delta m)$. In addition, we also restrict that detectable lenses should be brighter than a threshold magnitude of $I = 22$. For this computation, we assume that the source star has a fixed brightness of $M_I = 3.0$, which corresponds to that of a bulge clump giant, while the lens brightness is deduced from its mass by using the mass-luminosity relation provided by Kroupa, Tout & Gilmore (1993). Once the absolute magnitudes of the source and the lens are set, their apparent magnitudes

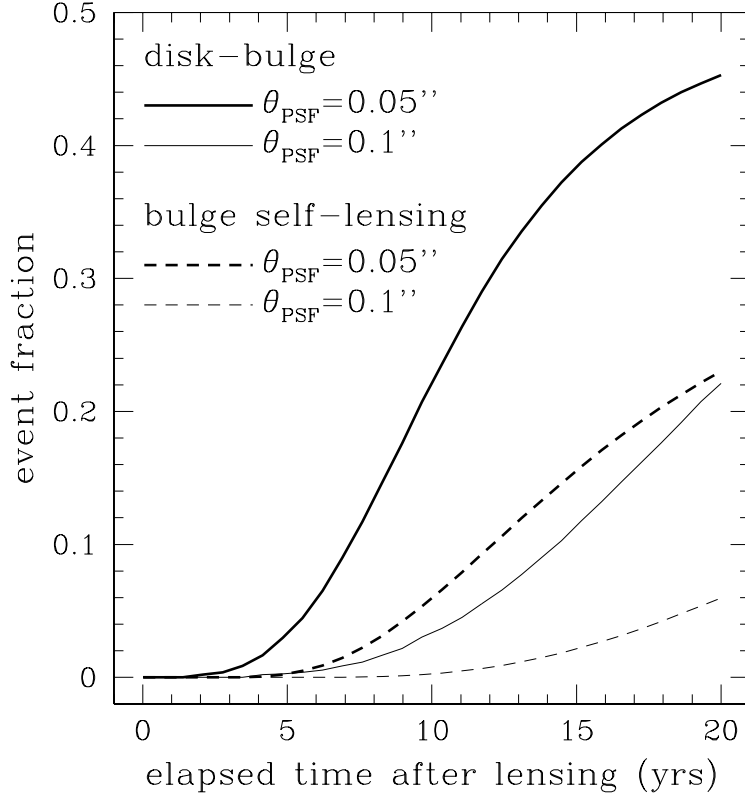


Figure 4. The fractions of events with lens-source separations $\Delta\theta = \mu\Delta t \geq \Delta\theta_{\text{th}}$ as a function of elapsed time after lensing magnification Δt . To estimate the fraction the actual minimum separation is considered due to the difference in magnitude for a given θ_{PSF} . The two pairs of curves drawn by continuous lines and dashed lines correspond to the fractions obtained with two different PSF separation of $\Delta\theta_{\text{PSF}} = 0''.05$ and $0''.1$. The red curves are for disk-bulge events while the blue curves are for bulge-bulge events.

are computed considering their distances from the observer, i.e. D_{OS} for the source and D_{OL} for the lens.

In Figure 4, we present the finally determined fractions of events with detectable lenses as a function of Δt . In the figure, the thick and thin curves represent the expected fractions when followup observations are conducted by using instruments with $\theta_{\text{PSF}} = 0''.05$ and $0''.1$, respectively. If the instrument has a resolution of $\theta_{\text{PSF}} = 0''.1$, we estimate that lenses can be resolved for $\sim 3\%$ and 22% of disk-bulge events and for $\sim 0.3\%$ and 6% of bulge self-lensing events after $\Delta t = 10$ and 20 years, respectively. The fraction increases substantially with the increase of the resolving power. If followup observations are performed by using an instrument with $\theta_{\text{PSF}} = 0''.05$, we estimate that lenses can be resolved for $\sim 22\%$ and 45% of disk-bulge events and for $\sim 6\%$ and 23% of bulge self-lensing events after $\Delta t = 10$ and 20 years, respectively.

4 DISCUSSION

In the previous section, we estimated the fraction of Galactic bulge events for which one can directly image lenses from followup observations by using high resolution imaging instruments and presented the result as a function of a time after original lensing measurements. In this section, based on the result in the previous section we discuss some of the observational aspects of the future followup lensing observations aimed for direct lens imaging.

First, from the distributions in Fig. 4, we find that the proper choice of the instrument for the future high resolution followup lensing observations will be NGST. Bulge events has been reported since 1993 (Udalski et al. 1994; Alcock et al. 1995a). Under a rough assumption that disk-bulge and bulge self-lensing events equally contribute to the total Galactic bulge event rate and considering the life expectancy of HST, the fraction of events with resolvable lenses from HST observations will be just $\sim 5\%$ even if the followup observations are performed at the end stage of HST for the first generation of lensing events. However, by using NGST, which is scheduled to be launched in 2009, it will be possible to resolve lenses for a significant fraction of events.

Second, given that all lensing events will be unable to be followed up due to the limited observation time of NGST, priority of targets should be given to events from which one can obtain extra information about the lens or the source star other than the identification of the lens as a normal star and the measurement of the lens-source proper motion. As mentioned in § 1, one can measure the angular radius of the source star of an event, for which the source was previously resolved, and uniquely determine the lens mass of an event, for which the lens parallax was measured. Therefore, these events should be at the top of the target list. In the published literature, we find 10 events, for which the source star was well resolved (Alcock et al. 1997, 2000a; Albrow et al. 1999, 2000, 2001a,b; Afonso et al. 2000; An et al. 2002)[†], and 11 events, for which parallax effect was measured (Alcock et al. 1995b; Mao 1999; Soszyński et al. 2001; Smith, Mao, & Woźniak 2002). Another possible high priority targets will be the longest events with $t_E \gtrsim 70$ days. These events cannot be well explained by the standard models of the geometrical and kinematical distributions of lenses and their mass function (Han & Gould 1996). Although these events comprise a small fraction ($\lesssim 10\%$) of the total number of events, they are important because their contribution to the total optical depth is important. Detection of lenses and the measured proper motions (or non-detection of lenses) will allow one to better constrain the nature of these mysterious events.

[†] Among them, one event was detected towards the Small Magellanic Cloud (MACHO 98-SMC-1).

5 SUMMARY AND CONCLUSION

We have estimated the fraction of Galactic bulge microlensing events for which the lenses can be directly imaged from future high resolution followup observations by computing the distribution of proper motions of the currently detected bulge events and imposing realistic criteria for lens resolution. From this computation, we find that lens identification will be possible for a significant fraction of bulge events from followup observations using NGST under the assumption that most bulge events are caused by normal stars. Besides identifying lenses as stars, direct lens imaging will allow one to accurately determine the lens proper motion, from which the physical parameters of the individual lenses can be better constrained. If lenses are imaged for events where lens parallaxes were measured, the lens parameter degeneracy can be completely broken and the lens mass can be uniquely determined. In addition, high resolution followup observations will provide a valuable chance to measure the angular radii of remote bulge source stars involved with events for which the source was previously resolved via either a source transit or a caustic crossing.

We would like to thank A. Gould for proving useful comments about the work. This work was supported by a grant (R01-1999-00023) of the Korea Science & Engineering Foundation (KOSEF).

REFERENCES

- Afonso, C. et al., 2000, ApJ, 532, 340
 Alard C., Guibert J., 1997, A&A, 326, 1
 Albrow M. D. et al., 1999, ApJ, 522, 1011
 Albrow M. D. et al., 2000, ApJ, 534, 894
 Albrow M. D. et al., 2001a, ApJ, 549, 759
 Albrow M. D. et al., 2001b, ApJ, 550, L173
 Alcock C. et al., 1993, Nature, 365, 621
 Alcock C. et al., 1995a, ApJ, 445, 133
 Alcock C. et al., 1995b, ApJ, 454, L125
 Alcock C. et al., 1997, ApJ, 491, 436
 Alcock C. et al., 2000a, ApJ, 541, 270
 Alcock C. et al., 2000b, ApJ, 541, 734
 Alcock C. et al., 2001, Nature, 414, 617
 Alonso A., Salaris M., Arribas S., Martinez-Roger C., Asensio Ramos A., 2000, A&A, 355, 1060
 An J. A. et al., 2002, ApJ, 572, 521
 Aubourg E. et al., 1993, Nature, 365, 623
 Bahcall J. N., 1986, ARA&A, 24, 577
 Binney J., Tremaine S., 1987, Galactic Dynamics (Princeton: Princeton Univeristy Press), 67
 Blum R. D., 1995, ApJ, 444, L89
 Bond I. et al., 2001, MNRAS, 327, 868
 Dwek E. et al., 1995, ApJ, 445, 716
 Evans N. W., Belokurov V., 2002, ApJ, 567, L119
 Evans N. W., Collett J. L., 1993, MNRAS, 264, 353
 Gould A., 1994, ApJ, 421, L71
 Gould A., 2001, PASP, 113, 903

- Han C., Gould A., 1995, ApJ, 447, 53
 Han C., Gould A., 1996, ApJ, 467, 540
 Kroupa P., Tout C. A., Gilmore G., 1993, MNRAS, 262, 545
 Mao S., Paczyński B., 1996, ApJ, 473, 57
 Mao S. 1999, A&A, 350, L19
 Nemiroff R. J., Wickramasinghe W. A. D. T., 1994, ApJ, 424, L21
 Paczyński B., 1986, ApJ, 304, 1
 Smith M. C., Mao S., Woźniak P., 2002, MNRAS, 332, 962
 Soszyński I. et al., 2001, ApJ, 552, 731
 Udalski A., Szymanski M., Kaluzny J., Kubiak M., Krzeminski W., Mateo M., Preston G. W., Paczynski, B. 1993, Acta Astron., 43, 289
 Udalski A., Szymanski M., Kaluzny J., Kubiak M., 1994, Acta Astron., 44, 1
 Witt H. J., Mao S., 1994, ApJ, 430, 505